NOLTA, IEICE

Paper

Reversal-time dynamics of two-dimensional non-autonomous systems

Michiru Katayama [1] *Tetsushi Ueta* [2]

[1] *Anan National College of Techonology*
Minobayashi, Anan, Tokushima 774-0017, Japan

[2] *Tokushima University*
2-1, Minami-Josanjima, Tokushima 770-8506, Japan

Received August 9, 2024; Revised October 7, 2024; Published January 1, 2025

Abstract: This study, we discusses the topological type of nonautonomous systems with periodic solutions when the time variable t increases negatively. When linear approximation holds near a fixed point of the Poincaré map, we confirm that the bifurcation points where the fixed point becomes nonhyperbolic are invariant regardless of the time direction however, the stability of the fixed point is changed. Consequently, we show that two-dimensional bifurcation diagrams obtained by the brute-force method give different results for positive and reversal-time variable systems; however, the bifurcation curves are identical. The inverted time variable system is useful for visualizing the completely unstable fixed point, because the repeller can be observed as an attractor. Furthermore, in certain models, chaotic attractors with a wide parameter range exist in reversal time variable systems.

Key Words: bifurcation, chaos, reversal-time, diode

1. Introduction

Discovering nonlinear systems with chaotic attractors is a significant achievements in the development of chaos theory. Various types of chaos have been discovered, such as the Duffing-Rayleigh [1] equation as a differential equation for nonautonomous systems and the Lorenz [2] and Rossler [3] equations as autonomous systems. Distinguishing between such nonlinear systems is necessary to discuss the essential components of chaos and its applications. Numerical analysis of the created model is a basic technique in studying such systems. When performing numerical analysis of differential equations, a time variable, t, is often chosen as an independent variable. This variable is usually a non-negative, but it becomes a time reversal if negative. Here, we define the case where the time variable is positive as a forward time system and the system where the time variable is negative as a reversal-time system.

In previous research on reversal-time, Roberts et al. [4] and Lamb et al. [5] summarized their research on systems with time-reversal symmetry. Hoover et al. [6] indicated that the symmetry of

  DOI: 10.1587/nolta.16.147

the Lyapunov exponent is broken even in systems with time-reversal symmetry. Huh et al. [7] also expanded the concept of time-reversal symmetry by creating a loss function that indicates the degree to which time-reversal symmetry is maintained. Furthermore, Sprott et al. [8] discussed the properties of the equations corresponding to time reversal for the Lorentz equations. Moreover, Hou et al. [9] showed that when time reversal occurs, it is topologically inequivalent to a system with positive time variables, adding that the flow direction is generally not preserved. However, they showed that the repeller and attractor are chaotic in the limit set where each time variable diverges to infinity.

This study investigates the correspondence between the topilogical types of two systems with different signs of time variables, as discussed by Sprott et al. [8] To achieve this, we first discuss the case near the fixed point of the Poincaré map. We then discretize these periodic solutions using the Poincaré map and classify the linear approximation region near the fixed point. From these results, we discuss the correspondence of topological types between two systems with different signs of time variables. Next, we define forward time and reversal-time systems for an electric circuit model and analyze the topological properties of the waveforms through numerical calculations. We then create bifurcation diagrams for both forward and reversal times, confirming that the contents discussed in the linear approximated region near the fixed point can be observed.

2. Fixed point and its stability with forward/reversal-time

Let us consider a two-dimensional nonautonomous system:

$$\frac{d\boldsymbol{x}}{dt} = \boldsymbol{f}(\boldsymbol{x}, \lambda) + \boldsymbol{g}(t), \tag{1}$$

where, $\boldsymbol{x} \in \boldsymbol{R}^2$ is a state, $\boldsymbol{f}$ is a C^∞ class function, $\lambda \in \boldsymbol{R}$ is a parameter, and $\boldsymbol{g}(t)$ is a periodic function satisfying $\boldsymbol{g}(t) = \boldsymbol{g}(t+\tau)$ and $\boldsymbol{g}(-t) = \boldsymbol{g}(t)$. By substituting $-t$ for t, we have the following:

$$\frac{d\boldsymbol{x}}{dt} = -\boldsymbol{f}(\boldsymbol{x}, \boldsymbol{\lambda}) - \boldsymbol{g}(t). \tag{2}$$

We can study Eq. (2) to analyze the reversal-time behavior of Eq. (1). If we define the solution function of Eq. (1) as $\boldsymbol{x}(t) = \phi(t, \boldsymbol{x}, \lambda)$, the periodic solution can be expressed as follows:

$$\boldsymbol{\phi}(t+\tau, \boldsymbol{x}^*, \lambda) = \boldsymbol{\phi}(t, \boldsymbol{x}^*, \lambda),\ \forall t \in \boldsymbol{R}, \tag{3}$$

where $\boldsymbol{x}^*$ is the initial value of the periodic solution, and τ is the period. Equations (1) and (2) are two-dimensional nonautonomous systems subjected to periodic external forces with period 2π; therefore, we define the Poincaré map T as follows:

$$\begin{aligned} &T : \boldsymbol{R}^2 \to \boldsymbol{R}^2; \\ &\quad \boldsymbol{x}_k \mapsto \boldsymbol{x}_{k+1} = T(\boldsymbol{x}_k) = \boldsymbol{\phi}(2\pi(k+1), \boldsymbol{x}_k, \lambda), \end{aligned} \tag{4}$$

where $\boldsymbol{x}_k \equiv \boldsymbol{x}(2\pi k) = \phi(2\pi k, \boldsymbol{x}, \lambda)$, $k = 0, 1, 2, \cdots$ are the discretized state variables.

If one observes a periodic solution for Eq. (1), we obtain

$$\boldsymbol{x}_{k+1} = T(\boldsymbol{x}_k) \tag{5}$$

by applying the Poincaré mapping, whose period is 2π. The fixed point of Eq. (1) is also the fixed point of Eq. (2). Because for Eq. (5), we derive $\boldsymbol{x}(k-1) = T^{-1}(\boldsymbol{x}(k))$, i.e., $\boldsymbol{x}^* = T(\boldsymbol{x}^*) = T^{-1}(\boldsymbol{x}^*)$.

Here, we discuss the topological types of the difference equation by the Poincaré map. For the subspace obtained by the Poincaré map, the state variables around the fixed point are set as $\boldsymbol{\xi}_k = (\xi_{k,1}, \xi_{k,2})$. The characteristic multipliers of each eigenvector are set as μ_1 and μ_2. Table I shows all topological types of fixed points for Eq. (5). The leading number of the symbol shows the number of multipliers whose absolute value is bigger than unity. ${}_1D$ has an unstable manifold whose mapping direction is preserved, and ${}_1I$ has an unstable manifold whose mapping direction is flipped for each iteration. For a more detailed explanation of the topological classification of the fixed point, see Kawakami [10].

Table I. Stability of fixed points in Eq. (5).

Symbol	condition	name	stability
${}_0D$	$\lvert\mu_1\rvert < 1, \lvert\mu_2\rvert < 1$	sink	completely stable
${}_1D$	$0 < \mu_1 < 1 < \mu_2$	saddle	one dimensionally unstable
${}_1I$	$\mu_1 < -1 < \mu_2 < 0$	saddle	one dimensionally unstable
${}_2D$	$\lvert\mu_1\rvert > 1, \lvert\mu_2\rvert > 1$	source	completely unstable

Suppose that both multipliers are real. Then, the local activity about the fixed point is written by $\boldsymbol{\xi}_{k+1,j} = \mu_j \boldsymbol{\xi}_{k,j}$, where, $\boldsymbol{\xi}_{k,j}$ is an eigenvector correspoinding to the eigenvalue $\mu_j, j = 1, 2$. An activity on a subspace $\boldsymbol{\xi}$ is written by $\boldsymbol{\xi}_{k+1,j} = \mu_1 \boldsymbol{\xi}_{k,j}$. For the reversal-time, this leads to $\boldsymbol{\xi}_{k+1,j} = \boldsymbol{\mu}_1^{-1} \boldsymbol{\xi}_{k,j}$, i.e., the stability of the subspace is flipped. If the multipliers are $a \pm ib$, where $i = \sqrt{-1}$, a and b are real numbers. The linearized space about the fixed point can be described as

$$\begin{pmatrix} \xi_{k+1,1} \\ \xi_{k+1,2} \end{pmatrix} = \begin{pmatrix} a & -b \\ b & a \end{pmatrix} \begin{pmatrix} \xi_{k,1} \\ \xi_{k,2} \end{pmatrix} = r \begin{pmatrix} \cos\theta & -\sin\theta \\ \sin\theta & \cos\theta \end{pmatrix} \begin{pmatrix} \xi_{k,1} \\ \xi_{k,2} \end{pmatrix},$$

where, $r = \sqrt{a^2 + b^2} > 0$, and $\theta = \arctan(b/a)$. Thus, we have

$$\begin{pmatrix} \xi_{k-1,1} \\ \xi_{k-1,2} \end{pmatrix} = r^{-1} \begin{pmatrix} \cos\theta & \sin\theta \\ -\sin\theta & \cos\theta \end{pmatrix} \begin{pmatrix} \xi_{k,1} \\ \xi_{k,2} \end{pmatrix}.$$

The stability is flipped against $r = 1$; therefore, ${}_0D$ in the forward time corresponds to ${}_2D$ in the reversal-time. While, ${}_1D$ and ${}_1I$ in the forward time are still saddled toward the reversal-time; however, the stabilities of both eigenspaces are exchanged.

Furthermore, a bifurcation of a periodic solution in Eq. (1) is also the same bifurcation in Eq. (2). Because, for the period-doubling or the tangent bifurcation, one of the multipliers should be $\mu = -1$ or $\mu = 1$, respectively. The inverse values of them are identical. For the Neimark–Sacker bifurcation, complex conjugate multipliers are on the unit circle (i.e., $e^{\pm i\theta}$, where $\theta \neq 0$ or $\theta \neq \pi$), and they are involutive of each other.

Since the fixed point remains the same regardless of the direction of time, tracking bifurcation sets for both positive and reversal time is very important to grasp the dynamical properties of the given system; however, only the forward time dynamics are usually analyzed. This paper provides an example that shows a wide variety of bifurcation structures for reversal-time dynamics. The structure deeply affects also forward time dynamic properties.

3. Topological classification of fixed points in a forward time system and their correspondence with reversal-time system

Here, we discuss topological classifications around fixed points in forward and reversal time. For simplicity, we discuss the bifurcation phenomena of codimension one.

3.1 Tangent bifurcation of fixed point

This bifurcation is one in which two pairs of fixed points collide and either disappear or are created. If the tangent bifurcation point is $\boldsymbol{\lambda}_t$, the topological type of the pair of fixed points around the bifurcation point can be described as follows:

$$\begin{cases} {}_0D + {}_1D & \text{if } \mu < 1 \\ \emptyset & \text{if } \mu > 1. \end{cases}$$
$$\begin{cases} {}_1D + {}_2D & \text{if } \mu < 1 \\ \emptyset & \text{if } \mu > 1. \end{cases} \tag{6}$$

Here, $\emptyset$ denotes the disappearance of two pairs of fixed points. μ represents either μ_1 or μ_2, which is an arbitrary characteristic multiplier at which bifurcation occurs. The hyperbolicity is lost when $\mu = 1$, so we will not discuss it here.

Table II. Stability of fixed points in time-reversed Eq. (5).

Symbol	condition	name	stability
${}_2D$	$\lvert\mu_1\rvert < 1, \lvert\mu_2\rvert < 1$	source	completely unstable
${}_1D$	$0 < \mu_2 < 1 < \mu_1$	saddle	one dimensionally unstable
${}_1I$	$\mu_2 < -1 < \mu_1 < 0$	saddle	one dimensionally unstable
${}_0D$	$\lvert\mu_1\rvert > 1, \lvert\mu_2\rvert > 1$	sink	completely stable

Consider the case of the above topological type in reversal-time. From the discussion in Chapter 2, the fixed point changes as μ_i^{-1}; Table II presents the stability of the fixed point changes, confirming that the sink and source are swapped. Note that the topological type of the hyperbolic fixed point does not change, but the stability of the characteristic multiplier is swapped; therefore, the state before and after bifurcation in Eq. (6) is swapped.

$$\begin{cases} {}_1D + {}_2D & \text{if } \mu > 1 \\ \emptyset & \text{if } \mu < 1. \end{cases}$$

$$\begin{cases} {}_0D + {}_1D & \text{if } \mu > 1 \\ \emptyset & \text{if } \mu < 1. \end{cases}$$

This situation means that the nature of the characteristic multipliers is swapped: the bifurcation of ${}_0D + {}_1D$ changes to ${}_1D + {}_2D$, and the converse is also true.

3.2 Period doubling bifurcation of fixed point

This bifurcation occurs when one of the characteristic multipliers crosses -1 due to a parameter change. Since this can occur in various topological types, the patterns of change are also diverse. Below, we specifically enumerate the topological types around bifurcation points in a 2-dimensional nonautonomous system:

$$\begin{cases} {}_1I + 2{}_0D^2 & \text{if } \mu > -1 \\ {}_0D & \text{if } \mu < -1 \end{cases}$$

$$\begin{cases} {}_1I + 2{}_2D^2 & \text{if } \mu > -1 \\ {}_2D & \text{if } \mu < -1 \end{cases}$$

$$\begin{cases} {}_2D + 2{}_1D^2 & \text{if } \mu > -1 \\ {}_1I & \text{if } \mu < -1 \end{cases}$$

$$\begin{cases} {}_0D + 2{}_1D^2 & \text{if } \mu > -1 \\ {}_1I & \text{if } \mu < -1. \end{cases}$$

Here, ${}_kD^2$, $k = 0, 1, 2$ denotes a 2-periodic point of topological type D with unstable dimension k. The coefficient 2 indicates that two periodic points occur. These topological types are interchanged in the forward-time system (2) in the same way as in the case of tangent bifurcation.

3.3 Neimark–Sacker bifurcation of fixed point

A characteristic multiplier expressed as $a \pm ib$ indicates a bifurcation that crosses the unit circle in the complex plane. The topological type around the bifurcation point is

$$\begin{cases} {}_2D + ICC & \text{if } \lvert\mu\rvert > 1 \\ {}_0D & \text{if } \lvert\mu\rvert < 1 \end{cases}$$

$$\begin{cases} {}_2D & \text{if } \lvert\mu\rvert > 1 \\ {}_0D + ICC & \text{if } \lvert\mu\rvert < 1. \end{cases}$$

Here, ICC represents an invariant closed curve, representing a torus in a continuous-time response. The former corresponds to a supercritical Hopf bifurcation at a fixed point, and the latter to a subcritical Hopf bifurcation. In the reversal-time system, the supercritical and subcritical are interchanged, as in the case of tangent bifurcation and period-doubling bifurcation.

In this way, the stability of the characteristic multiplier is switched in the reversal-time system, and the behavior on the Poincaré map changes to correspond to that of the forward time system. Therefore, the behavior of the forward time system can be predicted to some extent by analyzing the reversal-time system. Furthermore, since the fixed points are common, it is expected to be useful when obtaining bifurcation diagrams using the brute-force method.

4. Example of inverse time analysis: RLC circuit with inverse characteristic diode connected

In Section 3, we confirmed that although the bifurcation parameter remains the same between the forward and reversal-time systems, the topological properties are swapped around this parameter. This section confirms that the properties of Section 3 are indeed observed by visualizing the bifurcation sets for the forward and reversal-time systems defined in Section 2 with concrete examples.

A diode is modeled with an exponent function (Shockley ideal diode), a piecewise linear function, an ON/OFF switch, and so on. These models look simple; however, they contain many higher-order nonlinear terms. We expect this fact to cause nonlinear behavior, including various bifurcations and chaotic solutions.

Tanaka and Matsumoto [11] studied a forced RL-diode serial circuit. The parasite capacitance is modeled as a piecewise negative linear function, and charge and voltage of the capacitor are chosen as the state variables. Chaotic solutions via a period-doubling cascade are confirmed, and a one-dimensional map with suitable simplifications explains a chaotic behavior.

Against this, we use a plain capacitor and attach a diode in parallel to the capacitor, and the current and voltage of the capacitor are the state variables. This forced RLC-diode circuit does not have remarkable phenomenon because of the lack of active elements.

Figure 1 presents the target circuit, where a shaded area shows an inverted diode. An operational amplifier with this configuration inverts the characteristics of a diode located in the right corner. Therefore, suppose the diode is written by $I = I_s \exp \frac{qv}{\kappa T}$, where, I_s is the reverse-bias saturation current, q is an elementary charge, κ is the Boltzmann constant, T is the absolute temperature. In this case, the current of the shaded region gives $I = -I_s \exp \frac{qv}{\kappa T}$. The circuit equation is obtained from Kirchhoff's Current Law and Kirchhoff's Voltage Law as follows:

$$\begin{aligned} C\frac{dv}{dt} &= i + I_s \exp \frac{qv}{\kappa T}, \\ L\frac{di}{dt} &= -v - Ri + E_0 + E\cos \omega t \end{aligned} \tag{7}$$

By applying appropriate transformations, we have the normalized equation:

$$\begin{aligned} \dot{x} &= y + \exp \gamma x \\ \dot{y} &= -x - ky + B_0 + B\cos \tau, \end{aligned} \tag{8}$$

where a dot means $d/d\tau$. We fix $B_0 = -0.3$ and $B = 0.4$. The corresponding reversal-time system is obtained by $t \to -t$:

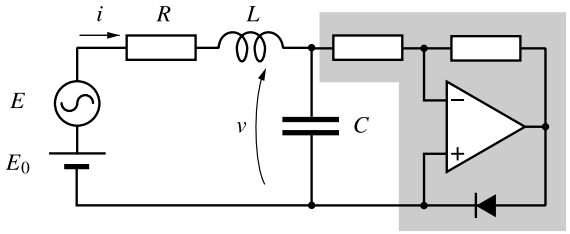

Fig. 1. An RCL circuit with an inverted diode.

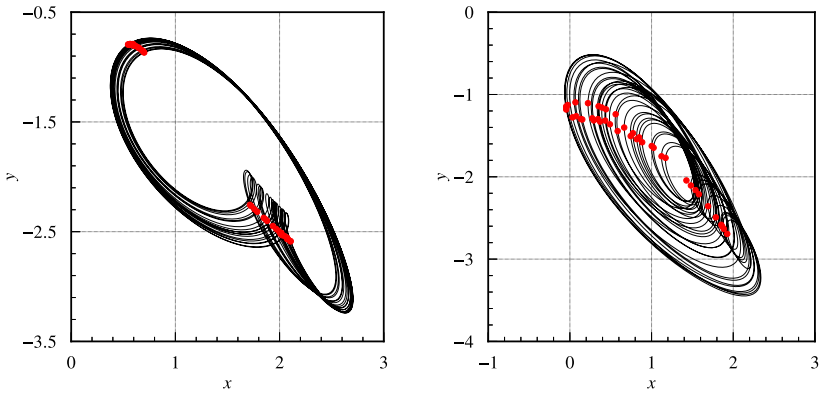

Fig. 2. Phase portraits of (a): Eq. (8), $\gamma = 0.42$, $k = 0.9398$. (b): Eq. (9), $\gamma = 0.501$, $k = 0.8$. The red circle is the Poincaré map of Eq. (4).

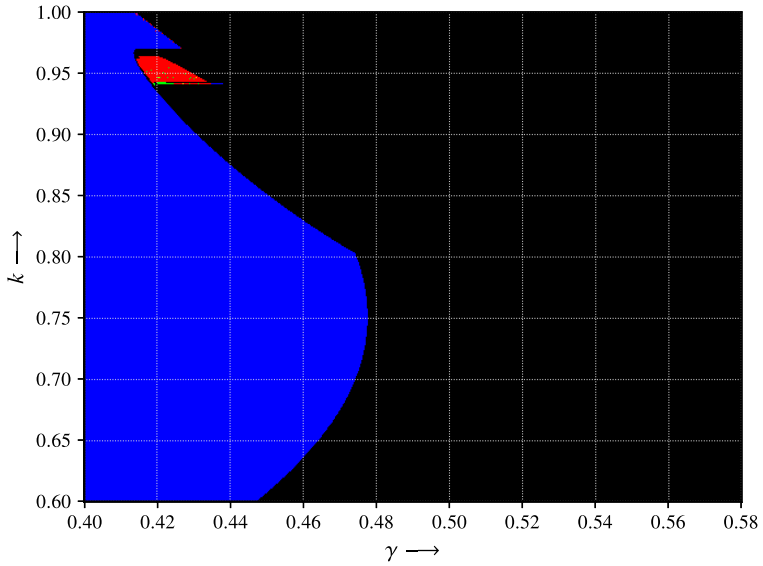

Fig. 3. Bifurcation diagram for a forward time system using only the brute-force method.

$$\begin{aligned} \dot{x} &= -y - \exp \gamma x \\ \dot{y} &= x + ky - B_0 - B \cos \tau. \end{aligned} \tag{9}$$

Figure 2 shows the respective phase diagrams. The red circle represents the Poincaré map of Eq. (4). Both systems exhibit chaos, but their stable regions are significantly different. Figure 3 shows a bifurcation diagram for forward-time systems using the brute-force method. The initial value is obtained by referring to the 1-periodic solution at the bottom left of the figure. A solution is found by shifting the value of γ by the increment, and then using the converged point as the initial value to find the adjacent point again. If it diverges, the previous initial value is inherited. When it reaches the right end, the value of k is increased, the initial value is inherited, and a similar search is performed from the left. Notably, due to these procedures, existing periodic solutions may not be drawn. The x-axis is the parameter γ, and the y-axis is the parameter k. The period of the periodic solutions is color-coded, and black regions are divergent or non periodic, including torus and chaos. At the same time, non-periodicity arises in forward time systems only in a small part of the areas where periodic solutions with periods of 2 or more are found, and most systems are divergent regions.

Figure 4 shows bifurcation diagrams of periodic points. By brute-force computations, colored areas corresponding to the period numbers are superimposed. In Fig. 4, G, I, and NS indicate tangent, period-doubling, and Neimark–Sacker bifurcations, respectively. The superscript shows the period, and the subscript is a nominal number. In Fig. 4(a), a period-doubling island exists, composed by $I_1^1 \cup I_2^1$. This island is connected with NS_1^1, NS_2^1, and NS^2. A set $NS_1^1 \cup I_1^1 \cup NS_2^1$ shows an edge

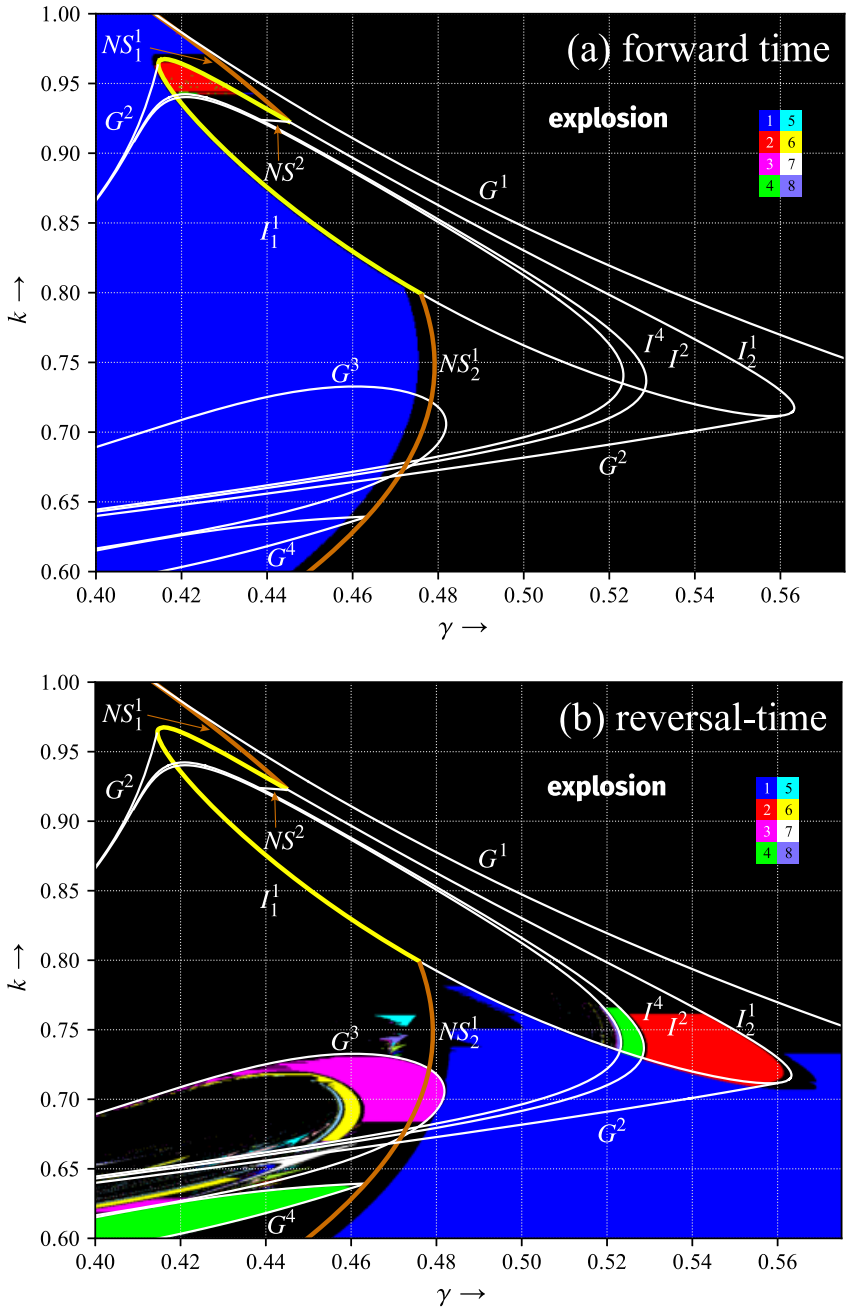

Fig. 4. Bifurcation diagrams of Eq. (8): (a) forward time, (b) reversal-time.

for the stable period-1 area. For NS^1, a sink turns to a source, and we generally have a stable ICC around this point; however, the solution diverges after an ICC-like transient. At the same time, I_1^1 gives two 2-period points and a saddle from a sink. Period-doubling cascades and chaotic solutions are confirmed in a very narrow parameter area. All stability is flipped in Fig. 4(b), but many entrainment regions like Arnold's tongues are obtained. Stable torus and chaos are given in a wide range of the parameter space.

Figure 6 shows the transient response of the forward and reversal-time systems at $\gamma = 0.47$ and $k = 0.75$. When the initial values x and y are set to 0.16 and -1.87, respectively, the phase diagram of the forward time system records the ranges of $0 < t < 500$, $100 < t < 500$ and $450 < t < 500$ from top to bottom. Figure 6 shows that the fixed point is stable, has a complex eigenvalue, and exhibits behavior suggesting an unstable ICC outside. Comparing with the bifurcation diagram reveals an NS bifurcation near this parameter, corresponding to the subcritical Hopf bifurcation of the fixed point in the forward time system. The right figures from the top two are for $0 < t < 500$ and $800 < t < 1000$,

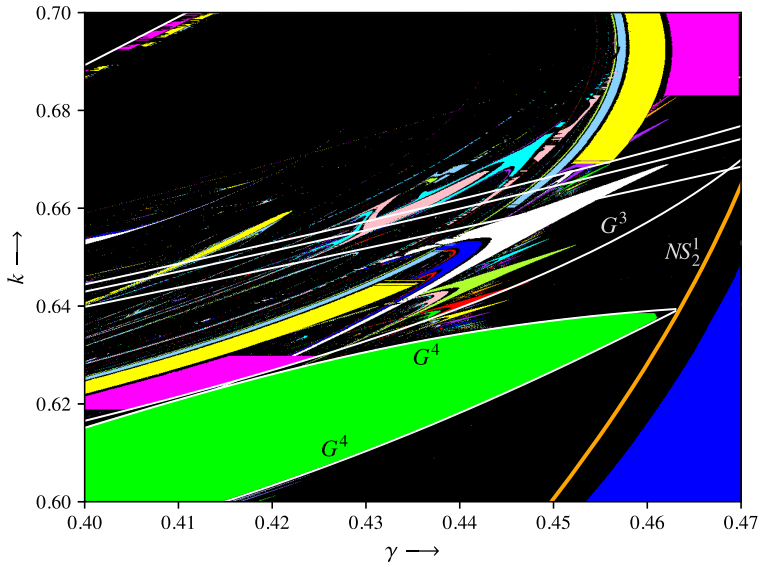

Fig. 5. bifurcation diagram for reversal-time systems.

and the bottom right figure shows the transient response in the $0 < t < 500$ range where the initial value is reset to the vicinity of a stable fixed point in the forward time system. The stable fixed point becomes an unstable fixed point after NS, a stable ICC is generated outside, and the phase locking has a period of 10. Therefore, this is an NS bifurcation corresponding to the supercritical Hopf bifurcation of the fixed point, and the behavior near the fixed point indeed switches between subcritical and supercritical in forward and reversal-time. We want to pay attention to the fact that phase locking can be observed in the behavior of the reversal-time system. Figure 5 shows an enlarged view of Fig. 4(b), showing that an Arnold tongue exists in the bifurcation structure. The phenomenon of phase synchronization in reverse time is a strange physical phenomenon. but The corresponding phenomenon in the forward time system has an unstable ICC; thus, using the brute-force method, the Arnold tongue does not exist near this fixed point and parameters.

Although the stabilities of the fixed points are different, the types of bifurcation are common to the forward time and reversal-time systems. This situation shows that observations in the reversal-time system help trace the bifurcation phenomenon of unstable fixed points using the brute-force method. Even when using the shooting method [10] to obtain bifurcation sets, detailed analysis is required to discover the existence of completely unstable periodic solutions. Therefore, the reversal-time system, in which volatile fixed points or unstable ICCs can be observed as stable, is an effective method for understanding the bifurcation structure of forward time systems.

5. Conclusion

This study used concrete analytical results to discuss the correspondence between forward time and reversal-time systems. We confirmed that the forward time and reversal-time systems share the fixed points corresponding to the discretization of the periodic solutions. Furthermore, the derivation of the bifurcation curves is equivalent to finding the fixed points of the forward and reversal-time systems. We also organized the topological types around the fixed points and organized the correspondence between the forward and reversal-time systems. These results showed that using the reversal-time system is helpful for simple analytical methods such as the brute-force method and that there are cases in which unstable fixed points can be visualized.

We also confirmed that chaos not observed in the forward time system might exist in the reversal-time system. These results show that the analysis of the reversal-time system is sometimes effective as an analytical method. In future work, we would like to analyze the topological types of the reversal-time system other than those fixed points and consider the reversal-time system in more general systems.

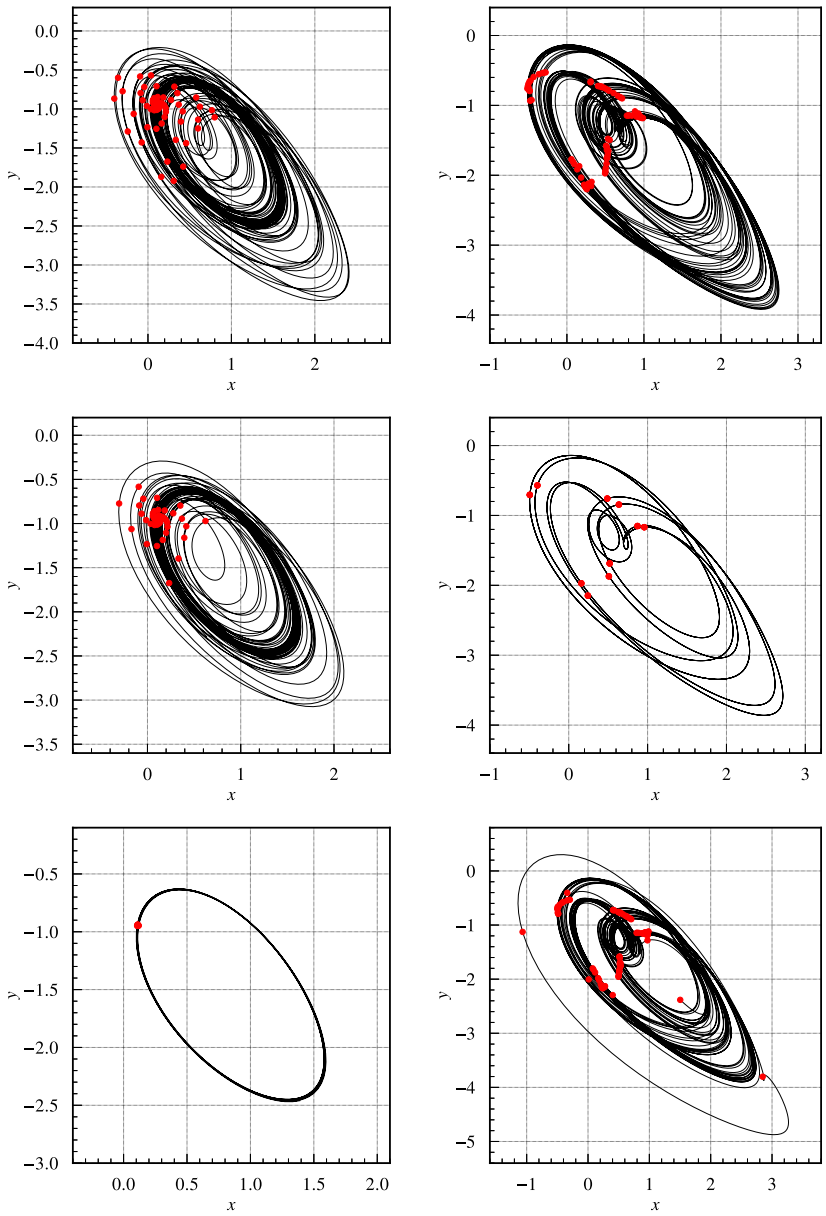

Fig. 6. Transient response of the phase diagram at $\gamma = 0.47$, $k = 0.75$. The red circle is the Poincaré map of Eq. (4). The left side corresponds to the forward time system, and the right side corresponds to the reversal time system.

Funding

This work has been supported by JSPS KAKENHI Grant Number 21K04109.

Conflicts of interest

The authors declare no competing interests.

Author contribution

Conceptualization:	T. U.
Funding acquisition:	T. U.
Investigation:	M. K., T. U.
Supervision:	T. U.
Visualization:	M. K., T. U.
Writing–original draft:	M. K., T. U.
Writing–review & editing:	M. K., T. U.

References

[1] K. Tsumoto, T. Ueta, T. Yoshinaga, and H. Kawakami, "Bifurcation analyses of nonlinear dynamical systems: From theory to numerical computations," *NOLTA*, vol. 3, no. 4, pp. 458–476, 2012.

[2] Edward N. Lorenz, "Deterministic Nonperiodic Flow," *Journal of the Atmospheric Sciences*, vol. 20, no. 2, pp. 130–141, 1963.

[3] O.E. Rössler, "An equation for continuous chaos," *Physics Letters A*, vol. 57, no. 5, pp. 397–398, 1976.

[4] J.A.G. Roberts and G.R.W. Quispel, "Chaos and time-reversal symmetry. Order and chaos in reversible dynamical systems," *Physics Reports*, vol. 216, no. 2–3, pp. 63–177, 1992.

[5] J.S.W. Lamb and J.A.G. Roberts, "Time-reversal symmetry in dynamical systems: A survey," *Physica D: Nonlinear Phenomena*, vol. 112, no. 1–2, pp. 1–39, 1998.

[6] W.G. Hoover, J.C. Sprott, and P.K. Patra, "Ergodic time-reversible chaos for Gibbs' canonical oscillator," *Physics Letters A*, vol. 379, no. 45–46, pp. 2935–2940, 2015.

[7] I. Huh, E. Yang, S.J. Hwang, and J. Shin, "Time-Reversal Symmetric ODE Network," *Advances in Neural Information Processing Systems 33*, pp. 19016–19027, 2020.

[8] J.C. Sprott, X. Wang, and G. Chen, "When Two Dual Chaotic Systems Shake Hands," *International Journal of Bifurcation and Chaos*, vol. 24, no. 6, p. 1450086, 2014.

[9] Z. Hou, N. Kang, X. Kong, G. Chen, and G. Yan, "On the nonequivalence of Lorenz system and Chen system," *International Journal of Bifurcation and Chaos*, vol. 20, no. 2, pp. 557–560, 2010.

[10] H. Kawakami, "Bifurcation of periodic responses in forced dynamic nonlinear circuits: Computation of bifurcation values of the system parameters," *IEEE Trans. circuits and systems*, vol. 31, no. 3, pp. 248–260, 1984.

[11] S. Tanaka, T. Matsumoto, and L.O. Chua, "Bifurcation scenario in a driven *R-L* diode circuit," *Phisica D*, vol. 28, no. 3, pp. 317–344, 1987.